Investigation of a Dual-Function Applicator for RF Hyperthermia and MRI

D. Yeo[1], X. Yang[2], J. Wu[3], L. W. Hofstetter[1], J. E. Piel[1], E. W. Fiveland[1], K. J. Park[1], and T. K. Foo[1]
[1]Imaging Technologies, GE Global Research, Niskayuna, NY, United States, [2]Power Conversion Circuits Lab, GE Global Research, Shanghai, China, People's Republic of, [3]Electrical and Computer Engineering, Northeastern University, Boston, MA, United States

Introduction: Clinical evidence indicates that adjuvant mild hyperthermia (41°C-43°C for 30-60 mins) of tumors significantly increases the effectiveness of radio- or chemo-therapy [1-3]. It is not designed to kill cancer cells directly but instead promotes drug and oxygen (radiosensitizer) diffusion through the dilated tumor vasculature. Deep-region heating can be induced by RF electric fields generated by multiple antennas. In a typical RF hyperthermia treatment planning session, a patient's MR/CT images are segmented and assigned values for electrical properties. EM simulations predict the antennas' E-field maps, which are used with electrical conductivity maps to optimize the antennas' phases and amplitudes to yield a desired SAR pattern. SAR is a first-order predictor of RF-induced temperature rise. Research RF hyperthermia systems typically use an applicator for heating (100-140MHz), and a 1.5T MR scanner (body coil) for MR thermometry. Inter-system cross-talk, oscillations [4], and low image SNR [5] have been reported. The applicator apparatus may also obstruct the use of small MR coil arrays, which could significantly improve acquisition speed (parallel imaging) and SNR (smaller coils closer to subject) of MR thermometry. To overcome these limitations, we reconfigure a MR loop coil array and assess its feasibility as a dual-function applicator for heating and imaging at the same frequency (127.74 MHz).

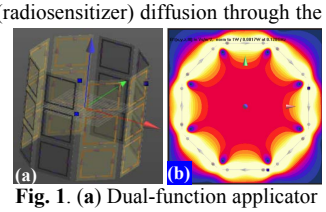

Fig. 1. (**a**) Dual-function applicator with C-type dipole antennas. (**b**) $|B_1|$ with azimuthal phases in loop

Method: It is well-known that a set of suitably arranged and tuned loop coils may receive and/or transmit RF for MRI (Fig. 1b). However, loop coils do not generate E-field radiation patterns amenable to deep region SAR steering. On the other hand, arrays consisting of straight dipole antennas with high power efficiencies are known to allow SAR steering for hyperthermia [1-3]. To enable imaging and heating with the same coil array, we reconfigured a tuned MR loop coil element into a C-shaped dipole antenna by removing two capacitors (loop capacitor and impedance matching capacitor) to form a lumped terminal loaded dipole antenna (Fig. 2a). In practice, the capacitors will be added or removed using fast RF switches to toggle between imaging (loop coil) and heating (C-shaped antenna) modes. The C-shaped dipole antenna was determined to have a radiation pattern similar to a strip dipole antenna (Fig. 2b,d). For the same antenna dimensions, the radiation efficiency of the C-shaped antenna can be higher due to a longer current path and capacitance load, making the effective antenna length closer to half a wavelength at 127.74 MHz. With EM simulations (SEMCAD X, SPEAG, Zurich, Switzerland), we drove the C-shaped antennas ((Fig. 2a) in a dual-function applicator (Fig 1a) with optimized phases and amplitudes to show that 3D SAR steering can be achieved (Fig. 3) in a cylindrical tissue phantom (ε= 63.495, σ=0.72 S/m , ρ=1040 kg/m3) [7]. We constructed a 4-element (10.5cm loop coils) array around a rigid deionized water bolus with an Agar phantom (94.8% DI H_2O, 4.5% Bacto Agar, 0.5% NaCl, 0.2% $CuSO_4$). A directional coupler was inserted before each C-shaped antenna's matching network and the phases and amplitudes were adjusted to be identical to those of a reference channel (phase combination A in Fig. 5b), i.e., signals fed into matching networks are identical. After heating for 45 mins with an average input power of 15W per channel, a phase difference PRFS MR thermometry map was acquired using a 3T GE MR750 scanner (GEHC, Waukesha, WI). Temperature maps were computed from spoiled gradient echo (SPGR) images acquired with scan parameters: TE = 12ms, TR = 100ms, flip angle = 35°, FOV = 48cm, matrix 128x128, axial 10mm slice, bandwidth 62.5kHz. After a cool-down period, C-shaped antenna 4's phase was incremented by 110° and another temperature map (Fig. 5c) was acquired after 45 mins of heating. The experiment was repeated for a strip dipole antenna-based applicator (Fig. 5d-f) in which strip dipole antenna 2's phase was varied instead (11.5cm long dipole antennas).

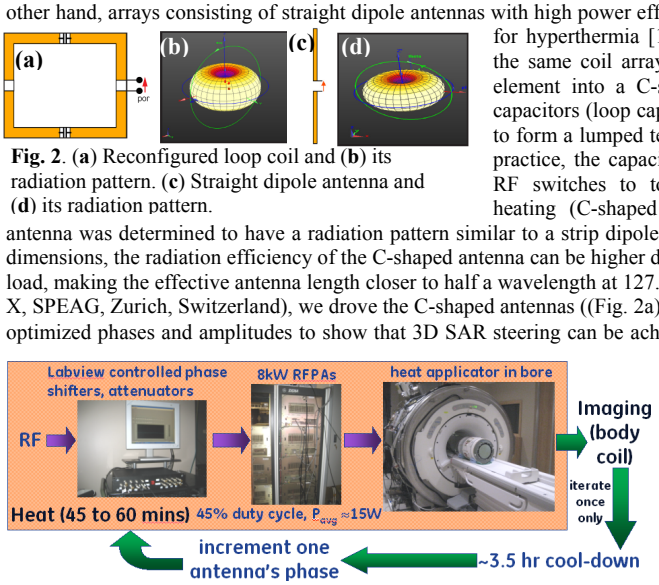

Fig. 2. (**a**) Reconfigured loop coil and (**b**) its radiation pattern. (**c**) Straight dipole antenna and (**d**) its radiation pattern.

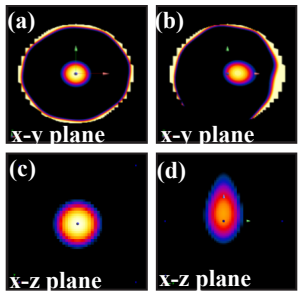

Fig. 3. SAR steering in (**a-b**) x-y and (**c-d**) x-z planes with optimized phase settings.

Fig. 4. Procedure of heating experiments for results in Fig. 5.

Results and Discussion: The experiments sought to determine if i) heating patterns can be varied by changing the C-shaped antennas' phases, ii) the C-shaped antennas' radiation efficiencies were sufficient to induce ~5°C temperature rise in <1 hr, and (iii) MR thermometry artifacts arose in the presence of the antennas. MR thermometry maps in Fig. 5b-c indicate an example where the heated region is varied by changing the phase of just one of the C-shaped antennas (CCW shift in heated region with +110° phase shift in antenna 4). The peak temperature rise was ≈4.3°C in 45 mins, which suggests the heating efficiency of the new design is adequate for mild hyperthermia. The heating patterns were repeatable in subsequent experiments. The isolation between C-shaped antennas 3 and 4 was high (S_{34}≈-21.3 dB), which strongly suggests that the spatial heat pattern shift was not due to inter-element coupling but to a change in the E-field interference pattern, which is the desired mechanism for SAR steering. There were no significant image artifacts in the Agar phantom although low spatial frequency B_0 drift was sometimes observed during long duration heating. A fat-referenced MR thermometry approach [6] with a fat-water Agar phantom will mitigate errors due to this B_0 drift. Inconsistent temperature maps were observed in the water bolus due to convection flow when the DI water is heated but this region is clinically unimportant. Similar results are obtained for the straight dipole antenna array in Fig. 5d-f.

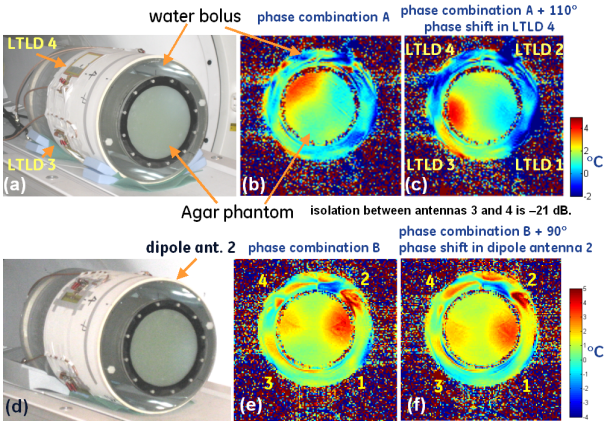

Fig. 5. (**a**) 4-element C-shaped antenna dual-function applicator with (**b**) initial temperature map (phase combination A) and (**c**) with antenna 4 phase shift. (**d**) Strip dipole antenna array with (**e**) initial temperature map and (**f**) with antenna 2 phase shift.

Conclusions: The results indicate that C-shaped dipole antenna arrays may perform steerable heating similar to straight dipole antenna arrays. Unlike the latter, however, the former is easily reconfigured into MR loop coils using RF switches, which could potentially enable 3D heat steering and MRI with the same physical applicator.

References
[1] Issels RD, et al. Lancet Oncology 2010;11:561-70. [2] Jones EL, et al. J Clin Oncol 2005;23:3079-085. [3] Franckena M, et al. Intl J Rad Oncol Biol Phys 2008; 70:1176-82. [4] Gellermann J, et al. Intl J Hyper 2008;24:327-35. [5] Stakhursky VL, et al. Phys Med Biol 2009;54:2131-2145. [6] Soher BJ et al. Magn Res Med 2010; 63:1238-1246. [7] Yang X, ISMRM 2011 (submitted).